Oxidation Kinetics of the Potent Insulin Mimetic Agent Bis(maltolato)oxovanadium(IV) (BMOV) in Water and in Methanol

Yan Sun,[1] Brian R. James, Steven J. Rettig, and Chris Orvig*

Medicinal Inorganic Chemistry Group, Department of Chemistry, University of British Columbia, Vancouver, BC, Canada V6T 1Z1

Received November 9, 1995[⊗]

The kinetics of oxidation of bis(maltolato)oxovanadium(IV), BMOV or $VO(ma)_2$, by dioxygen have been studied by UV−vis spectroscopy in both MeOH and H_2O media. The $VO(ma)_2$:O_2 stoichiometry was 4:1. In aqueous solution, the pH-dependent rate of the $VO(ma)_2/O_2$ reaction to generate *cis*-$[VO_2(ma)_2]^-$ is attributed to the deprotonation of coordinated H_2O, the deprotonated species $[VO(ma)_2(OH)]^-$ being more easily oxidized (k_{OH} = 0.39 M^{-1} s^{-1}, 25 °C) than the neutral form $VO(ma)_2(H_2O)$ (k_{H_2O} = 0.08 M^{-1} s^{-1}, 25 °C). The activation parameters for the two second-order reactions in aqueous solution were deduced from variable temperature kinetic measurements. In MeOH, $VO(ma)_2$ was oxidized by dioxygen to *cis*-$VO(OMe)(ma)_2$, whose structure was characterized by single-crystal X-ray diffraction; the crystals were monoclinic, $C2/c$, with a = 28.103(1) Å, b = 7.721(2) Å, c = 13.443(2) Å, β = 94.290(7)°, and Z = 8. The structure was solved by Patterson methods and was refined by full-matrix least-squares procedures to R = 0.043 for 1855 reflections with $I \geq 3\sigma(I)$. The kinetic results are consistent with a mechanism involving an attack of O_2 at the V(IV) center, followed by the formation of radicals and H_2O_2 as transient intermediates.

Introduction

Vanadium coordination chemistry has been of burgeoning interest since the discoveries of it being an essential trace element for certain organisms,[2,3] and as a cofactor in bromoperoxidase[4] and nitrogenases.[5] Our interest in vanadium chemistry and pharmacology has been largely stimulated by the insulin-mimetic properties of uncomplexed inorganic vanadate[6,7] and vanadyl,[8−10] as well as vanadyl complexes,[10−13] and the peroxovanadates.[14−16]

Bis(maltolato)oxovanadium(IV) (abbreviated BMOV or $VO(ma)_2$) was first designed in this laboratory to be an orally active insulin mimetic agent.[17−21] The choice of maltol as ligand was based on its bidentate monoprotic nature and on its ability to form metal complexes of moderated lipophilicity/hydrophilicity, as well as its nontoxicity (maltol is an FDA-approved food additive). The insulin-mimetic properties of $VO(ma)_2$ have shown it by *in vivo* studies to be roughly three times more effective than uncomplexed vanadyl sulfate.[21] This offers a significant step forward toward an oral treatment of diabetes.

Since the discovery of the insulin-mimetic effects of $VO(ma)_2$, we have extensively studied the structure and reactivity of this compound. The structure of $VO(ma)_2$ was characterized both in the solid state[22] and in various solutions.[22,23] In the solid state, $VO(ma)_2$ is five-coordinate with a square pyramidal geometry.[22] Coordination of a solvent molecule is seen upon dissolution of $VO(ma)_2$ under anaerobic conditions, the geometry of the six-coordinate V(IV) species being solvent dependent.[23] While stable to air in the solid state, $VO(ma)_2$ is oxidized in solution by O_2, and the products and rates of the oxidation reaction are also solvent dependent. Kinetic analyses of the $VO(ma)_2/O_2$ oxidation reactions in MeOH and in H_2O are reported in this paper.

Experimental Section

$VO(ma)_2$ and *cis*-$VO(OMe)(ma)_2$ were prepared as previously reported,[22] and their purities were confirmed by infrared spectroscopy, C/H elemental analyses (Mr. P. Borda, Department of Chemistry, UBC),

* To whom correspondence should be addressed. Tel: (604) 822-4449. FAX: (604) 822-2847. Internet: ORVIG@CHEM.UBC.CA.

⊗ Abstract published in *Advance ACS Abstracts,* February 1, 1996.

(1) Natural Sciences and Engineering Research Council of Canada Postdoctoral Fellow, 1994−1995.
(2) *Vanadium in Biological Systems*; Chasteen, N. D., Ed.; Kluwer: Dordrecht, The Netherlands, 1990.
(3) *Metal Ions in Biological Systems*; Sigel, H.; Sigel, A., Eds.; Marcel Dekker, Inc.: New York, 1995; Vol. 31.
(4) Vilter, H. *Phytochemistry* **1984**, *23*, 1387.
(5) Robson, R. L.; Eady, R. R.; Richardson, T. H.; Miller, R. W.; Hawkins, M.; Postgate, J. R. *Nature (London)* **1986**, *322*, 388.
(6) Fantus, I. G.; Kadota, S.; Deragon, G.; Foster, B.; Posner, B. I. *Biochemistry* **1989**, *28*, 8864.
(7) Kadota, S.; Fantus, I. G.; Deragon, G.; Guyda, H. J.; Posner, B. I. *J. Biol. Chem.* **1987**, *262*, 8252.
(8) Ramanadham, S.; Brownsey, R. W.; Cros, G. H.; Mongold, J. J.; McNeill, J. H. *Metabolism* **1989**, *38*, 1022.
(9) Ramanadham, S.; Mongold, J. J.; Brownsey, R. W.; Cros, G. H.; McNeill, J. H. *Am. J. Physiol.* **1989**, *257*, H904.
(10) Pederson, R. A.; Ramanadham, S.; Buchan, A. M. M.; McNeill, J. H. *Diabetes* **1989**, *38*, 1390.
(11) Sakurai, H.; Taira, Z.-E.; Sakai, N. *Inorg. Chim. Acta* **1988**, *151*, 85.
(12) Sakurai, H.; Tsuchiya, K.; Nukatsuka, M.; Kawada, J.; Ishikawa, S.; Yoshida, H.; Komatsu, M. *J. Clin. Biochem. Nutr.* **1990**, *8*, 193.
(13) Watanabe, H.; Nakai, M.; Komazawa, K.; Sakurai, H. *J. Med. Chem.* **1994**, *37*, 876.
(14) Shaver, A.; Ng, J. B.; Hall, D. A.; Soo Lum, B.; Posner, B. I. *Inorg. Chem.* **1993**, *32*, 3109.
(15) Posner, B. I.; Faure, R.; Burgess, J. W.; Bevan, A. P.; Lachance, D.; Zhang-Sun, G.; Fantus, I. G.; Ng, J. B.; Hall, D. A.; Soo Lum, B.; Shaver, A. *J. Biol. Chem.* **1994**, *269*, 4596.
(16) Shaver, A.; Hall, D. A.; Ng, J. B.; Lebuis, A.; Hynes, R. C.; Posner, B. I. *Inorg. Chim. Acta* **1995**, *229*, 253.
(17) McNeill, J. H.; Yuen, V. G.; Hoveyda, H. R.; Orvig, C. *J. Med. Chem.* **1992**, *35*, 1489.
(18) Yuen, V. G.; Orvig, C.; McNeill, J. H. *Can. J. Physiol. Pharmacol.* **1993**, *71*, 263.
(19) Yuen, V. G.; Orvig, C.; Thompson, K. H.; McNeill, J. H. *Can. J. Physiol. Pharmacol.* **1993**, *71*, 270.
(20) Dai, S.; Yuen, V. G.; Orvig, C.; McNeill, J. H. *Pharmacol. Commun.* **1993**, *3*, 311.
(21) Yuen, V. G.; Orvig, C.; McNeill, J. H. *Can. J. Physiol. Pharmacol.* **1995**, *73*, 55.
(22) Caravan, P.; Gelmini, L.; Glover, N.; Herring, F. G.; Li, H.; McNeill, J. H.; Rettig, S. J.; Setyawati, I. A.; Shuter, E.; Sun, Y.; Tracey, A. S.; Yuen, V. G.; Orvig, C. *J. Am. Chem. Soc.* **1995**, *117*, 12759.
(23) Sun, Y.; Hanson, G. R.; Orvig, C. To be submitted for publication.

0020-1669/96/1335-1667$12.00/0

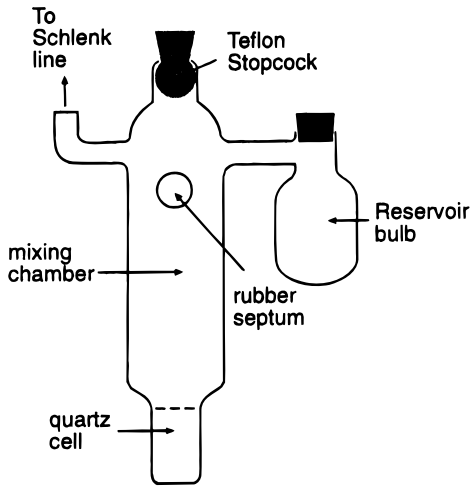

Figure 1. Quartz UV/vis cell with reservoir, mixing chamber, and Schlenk line attachment.

and solution ESR or ^{51}V NMR spectroscopies. HPLC grade MeOH was doubly distilled over CaH_2 under argon and subsequently underwent three cycles of freeze/pump/thaw degassing. Water was distilled (Barnstead D8902 and D8904 Cartridges), deionized (Corning MP-1 Megapure still), and further degassed either by freeze/pump/thaw or by bubbling through Ar. Hepes (4-(2-hydroxyethyl)-1-piperazineethanesulfonic acid) was used as obtained from Sigma.

Stock solutions of $VO(ma)_2$ in MeOH were made up anaerobically at room temperature using Schlenk techniques, and stored in Schlenk vials under N_2 or Ar at low temperature in powdered dry ice. Stock solutions thus prepared and stored were stable for at least 1 week, as verified by UV spectroscopy. Buffer solutions containing 50 mM Hepes were made in air, and the pH was adjusted with 1 or 2 N NaOH aqueous solutions. All the $VO(ma)_2$ aqueous solutions were freshly prepared prior to kinetic studies.

The O_2:V stoichiometries for the oxidation reactions were measured by following the O_2-uptake in a thermostated constant pressure apparatus which has been described previously.[24] ESR and ^{51}V NMR spectra (78.86 MHz) were employed to confirm the purity of the vanadium(IV) and vanadium(V) species, respectively, and were recorded on Bruker ECS-106 ESR and Varian XL-300 spectrometers.

Kinetic Measurements. The oxidation reactions of $VO(ma)_2$ in MeOH or H_2O under various conditions were monitored spectrophotometrically on a Shimadzu UV-2100 spectrometer in a thermostated (±0.2 °C) homemade anaerobic cell (Figure 1).[25] A quartz cell (1.0 cm) was attached to a reservoir by a side-arm, to a Teflon stopcock, and to an O-ring joint for connection to a Schlenk line fitted with a manometer. Reactions were studied under pseudo-first order conditions by employing a large excess of oxygen. Due to the difficulty in weighing precisely a small amount of solid $VO(ma)_2$ (~0.32 mg for each experiment), in a typical kinetic run in MeOH, 2 mL of a stock solution (0.5 mM $VO(ma)_2$, 10 mM maltol) was injected through a rubber septum into the quartz cell and the solvent was then removed under vacuum. MeOH (5 mL) was transferred to the reservoir and freeze/pump/thaw degassed; the apparatus was refilled with O_2 to a given pressure and equilibrated at 25 °C. The solvent and the solid $VO(ma)_2$ were then quickly mixed in the quartz cell. In aqueous solution studies, 100 mL of H_2O in a separate vial was degassed and saturated with O_2 at given pressure (0.2 or 1 atm) and temperature (18−40 °C). To this solution, $VO(ma)_2$ (19 mg, 0.06 mmol) and maltol (151 mg, 1.2 mmol) were added and the mixture was vigorously shaken; ~5 mL of this solution was then injected quickly to the anaerobic cell, which was preequilibrated at the same O_2 pressure and the same temperature. The reactions were monitored by the increased absorption at $\lambda = 448$ nm (λ_{max} for *cis*-$VO(OMe)(ma)_2$) in MeOH, and at $\lambda = 400$ nm (λ_{max} for *cis*-$[VO_2(ma)_2]^-$) in H_2O.

(24) James, B. R.; Mahajan, D. *Isr. J. Chem.* **1977**, *15*, 214.
(25) Barnabas, A. F.; Sallin, D.; James, B. R. *Can. J. Chem.* **1989**, *67*, 2009.

Table 1. Bond Lengths (Å) in *cis*-$VO(OMe)(ma)_2$

V(1)−O(2)	1.943(3)	V(1)−O(3)	2.121(3)
V(1)−O(5)	1.910(2)	V(1)−O(6)	2.252(2)
V(1)−O(7)	1.756(3)	V(1)−O(8)	1.590(2)
O(1)−C(2)	1.374(5)	O(1)−C(6)	1.331(6)
O(2)−C(3)	1.327(4)	O(3)−C(4)	1.268(4)
O(4)−C(8)	1.370(4)	O(4)−C(12)	1.342(5)
O(5)−C(9)	1.330(4)	O(6)−C(10)	1.263(4)
O(7)−C(13)	1.401(5)	C(1)−C(2)	1.474(6)
C(2)−C(3)	1.353(5)	C(3)−C(4)	1.421(5)
C(4)−C(5)	1.423(5)	C(5)−C(6)	1.334(6)
C(7)−C(8)	1.477(5)	C(8)−C(9)	1.352(5)
C(9)−C(10)	1.434(4)	C(10)−C(11)	1.424(5)
C(11)−C(12)	1.332(6)		

Pseudo-first-order rate constants k_{obs} were calculated from the slopes of plots of $\log(A_\infty - A_t)$ vs time by least-squares on the data of the first three half-lives, where A_t and A_∞ are the absorbances at time t and ∞, respectively. These plots were linear for at least three half-lives. Least-squares analyses of plots of k_{obs} vs $[O_2]$ were used to obtain the second-order rate constant k. The activation parameters for reactions in aqueous solutions were calculated from a least-squares analysis of the Eyring equations using two second-order rate constants k_{H_2O} and k_{OH}.

X-ray Crystallographic Analysis of *cis*-$VO(OMe)(ma)_2$. Crystals were isolated by slow evaporation of solvents from a *cis*-$VO(OMe)(ma)_2$ solution in a MeOH/MeCN mixture at room temperature. The final unit-cell parameters were obtained by least-squares on the setting angles for 25 reflections with $2\theta = 20.6-24.5°$. The intensities of three standard reflections, measured every 200 reflections throughout the data collection, remained constant. The data were processed[26] and corrected for Lorentz and polarization effects and absorption (empirical, based on azimuthal scans for three reflections).

The structure was solved by conventional heavy atom methods. The structure analysis was initiated in the centrosymmetric space group $C2/c$ on the basis of the E-statistics. This choice was confirmed by subsequent calculations. All non-hydrogen atoms were refined with anisotropic thermal parameters. Hydrogen atoms were fixed in calculated positions (C−H = 0.98 Å, $B_H = 1.2B_{bonded\ atom}$, methyl group orientations based on difference map peaks). Neutral atom scattering factors for all atoms[27] and anomalous dispersion corrections for the non-hydrogen atoms[28] were taken from the *International Tables for X-Ray Crystallography*. Bond lengths and bond angles appear in Tables 1 and 2, respectively. Complete crystallographic data, atomic coordinates and equivalent isotropic thermal parameters, hydrogen atom parameters, anisotropic thermal parameters, torsion angles, intermolecular contacts, and least-squares planes are included as Supporting Information (see paragraph at the end of paper).

Results

Oxidation of $VO(ma)_2$ in MeOH. Recently, we were able to grow crystals of $VO(ma)_2$ suitable for X-ray structure analysis.[22] In the solid state, $VO(ma)_2$ is five-coordinate with a square pyramidal geometry in which the oxo ligand occupies the axial position, and the two maltol ligands are trans to one another (Chart 1);[22] however, in a polar solvent such as MeOH or H_2O, a solvent molecule binds at a position primarily *cis* to the oxo ligand (Chart 1, cis isomer) as characterized previously by solution ESR spectroscopy.[23] Although VO^{2+} forms a stable 1:2 complex with maltol ($\log K_1 = 8.80(2)$, $\log K_2 = 7.51(2)$[22]), at low concentration, ligand dissociation processes are indicated by solution ESR spectra[23] (Scheme 1, left).

When a solution of $VO(ma)_2$ in MeOH is exposed to molecular oxygen or air, the oxidation is apparent from a

(26) *teXsan: Crystal Structure Analysis Package*; Molecular Structure Corporation: The Woodlands, TX, 1985 & 1992.
(27) *International Tables for X-Ray Crystallography*; Kynoch Press: Birmingham, England, 1974; Vol. IV, p 99.
(28) *International Tables for Crystallography*; Kluwer Academic Publishers: Boston, MA, 1992; Vol. C, p 200.

Table 2. Bond Angles in *cis*-VO(OMe)(ma)$_2$

O(2)−V(1)−O(3)	78.1(1)	O(2)−V(1)−O(5)	157.8(1)
O(2)−V(1)−O(6)	85.9(1)	O(2)−V(1)−O(7)	91.6(1)
O(2)−V(1)−O(8)	101.3(1)	O(3)−V(1)−O(5)	84.0(1)
O(3)−V(1)−O(6)	77.53(9)	O(3)−V(1)−O(7)	160.4(1)
O(3)−V(1)−O(8)	97.1(1)	O(5)−V(1)−O(6)	77.52(9)
O(5)−V(1)−O(7)	101.5(1)	O(5)−V(1)−O(8)	93.8(1)
O(6)−V(1)−O(7)	85.1(1)	O(6)−V(1)−O(8)	170.1(1)
O(7)−V(1)−O(8)	101.3(1)	C(2)−O(1)−C(6)	120.5(3)
V(1)−O(2)−C(3)	116.8(2)	V(1)−O(3)−C(4)	112.5(3)
C(8)−O(4)−C(12)	119.8(3)	V(1)−O(5)−C(9)	118.7(2)
V(1)−O(6)−C(10)	109.3(2)	V(1)−O(7)−C(13)	128.4(3)
O(1)−C(2)−C(1)	114.0(4)	O(1)−C(2)−C(3)	118.9(4)
C(1)−C(2)−C(3)	127.0(5)	O(2)−C(3)−C(2)	123.6(4)
O(2)−C(3)−C(4)	115.8(3)	C(2)−C(3)−C(4)	120.6(4)
O(3)−C(4)−C(3)	116.4(4)	O(3)−C(4)−C(5)	125.4(4)
C(3)−C(4)−C(5)	118.2(4)	C(4)−C(5)−C(6)	117.1(4)
O(1)−C(6)−C(5)	124.5(4)	O(4)−C(8)−C(7)	113.4(3)
O(4)−C(8)−C(9)	120.1(3)	C(7)−C(8)−C(9)	126.5(3)
O(5)−C(9)−C(8)	122.2(3)	O(5)−C(9)−C(10)	116.9(3)
C(8)−C(9)−C(10)	120.9(3)	O(6)−C(10)−C(9)	117.4(3)
O(6)−C(10)−C(11)	126.3(3)	C(9)−C(10)−C(11)	116.3(4)
C(10)−C(11)−C(12)	119.3(4)	O(4)−C(12)−C(11)	123.6(4)

Chart 1. Structures of VO(ma)$_2$ in the Solid State[22] and in Anaerobic MeOH or H_2O Solutions[23] (S = Solvent)

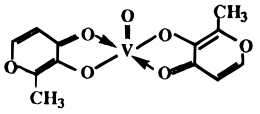

VO(ma)$_2$, BMOV

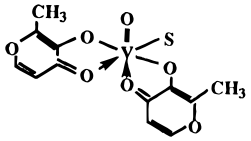

cis, major

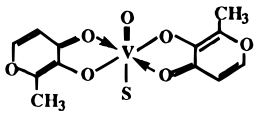

trans, minor

Scheme 1. Possible Behavior of VO(ma)2 in Aerobic MeOH Solution (Coordinated Solvent Omitted)

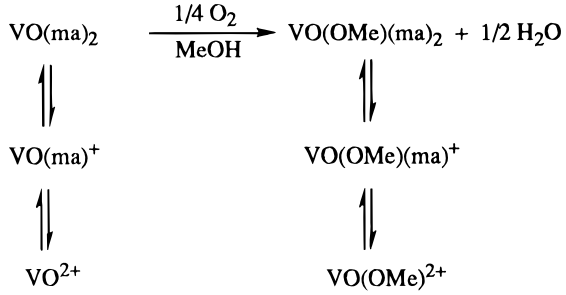

darkening of the color from pale yellow to red. The resulting oxidized solution contains three vanadium(V) species, as indicated by three well separated resonances in the ^{51}V NMR spectrum (Figure 2a); the major product has been isolated and identified as *cis*-bis(maltolato)(methoxo)oxovanadium(V) (^{51}V $\delta = -421$ ppm, *vide infra*). When pure crystalline VO(OMe)(ma)$_2$ is dissolved in MeOH, the ^{51}V resonance at −421 ppm is also joined by two extra peaks at −448 and −547 ppm; these are assigned to the ligand dissociation products, [VO(OMe)(ma)]$^+$ and [VO(OMe)]$^{2+}$, respectively (Scheme 1, right), and consistent with this, both peaks were completely suppressed by the addition of excess maltol (Figure 2b). This ligand dissociation process was first deduced from nonlinearity in the pseudo-first-order kinetic plots, and was also indicated by a severe deviation from Beer's law for VO(OMe)(ma)$_2$ (measured at λ_{max} = 448 nm). A 20-fold excess of maltol was sufficient to ensure the presence of of a single vanadium species for both the +4 and +5 oxidation states in solution when the total vanadium concentration was ≥0.2 mM. Under these conditions ([VO(ma)$_2$] = 0.2 mM; [maltol] = 4 mM), the oxidation of VO(ma)$_2$ by excess molecular oxygen was nicely pseudo-first order (*vide infra*). In the presence of 20-fold excess maltol, the VO(ma)$_2$:O$_2$ stoichiometry was 4:1.

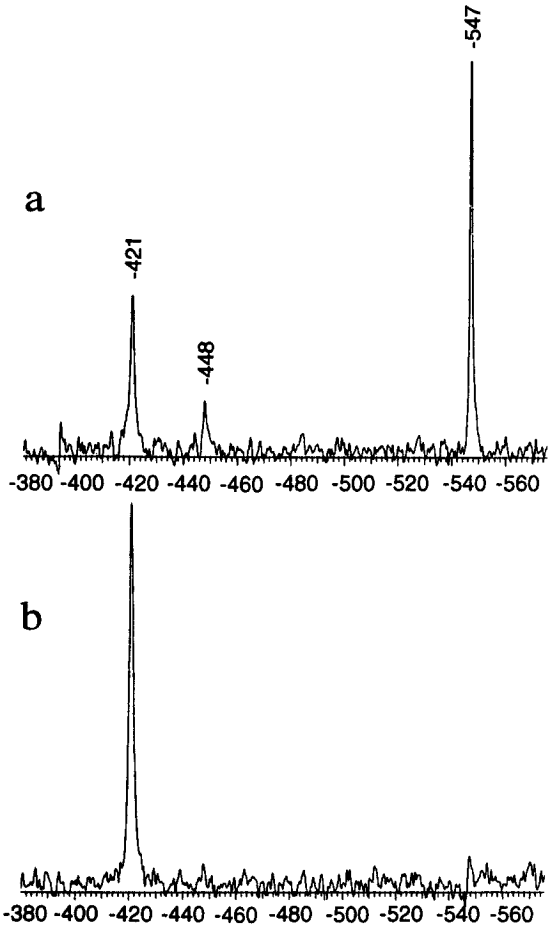

Figure 2. ^{51}V NMR spectra in MeOH/O$_2$: (a) [VO(ma)$_2$] = 0.5 mM; (b) [VO(ma)$_2$] = 0.5 mM; [maltol] = 10 mM.

Structure of *cis*-VO(OMe)(ma)$_2$. The numbering system and the molecular structure of *cis*-VO(OMe)(ma)$_2$ are shown in Figure 3. Bond lengths and angles are provided in Tables 1 and 2, respectively. The vanadium atom is octahedrally complexed to the oxo ligand, the methoxo ligand, and two ketonic and two alkoxo oxygen atoms of the two maltolato ligands. The oxo and methoxo ligands are cis to one another, which is a common feature for complexes bearing these two "strong" trans (π-bonding) ligands. The preference of strong π-bonding ligands for a cis configuration in such complexes has been demonstrated[29] recently in VO(OMe)(L) compounds (L= the tetradentate Schiff bases *N*,*N*′-2,2-dimethyltrimethylenebis[salicylideneaminate(2−)] (salnptn) and *N*,*N*′-ethylenebis[salicylideneaminate(2−)] (salen)), where the normally planar tetradentate Schiff base ligands were forced into three equatorial and one axial coordination positions to allow a *cis*-VO(OMe) arrangement.

The two ketonic oxygen atoms, not the two hydroxo oxygen atoms, are trans to oxo and methoxo ligands, respectively, consistent with the stronger field hydroxy oxygens having a strong orbital overlap with the vanadyl V; a similar coordination environment was found in the closely related structure of K[VO$_2$-

(29) Fairhurst, S. A.; Hughes, D. L.; Kleinkes, U.; Leigh, G. J.; Sanders, J. R.; Weisner, J. *J. Chem. Soc., Dalton Trans.* **1995**, 321.

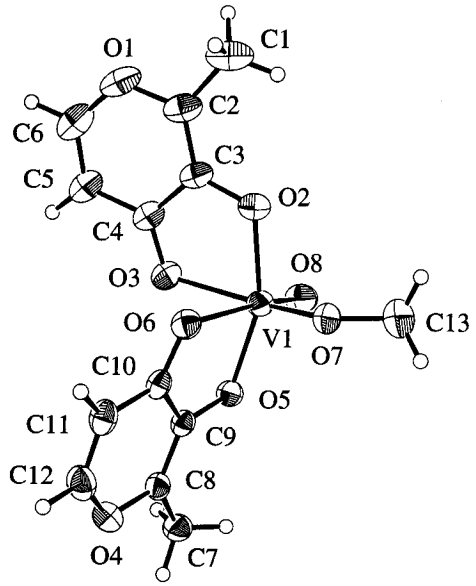

Figure 3. ORTEP diagram of *cis*-VO(OMe)(ma)$_2$. Thermal ellipsoids for the non-hydrogen atoms are drawn at the 33% probability level.

(ma)$_2$]·H$_2$O,[22] and in related bis(8-hydroxyquinolinato)(isopropoxo)oxovanadium(V) complexes, where the amino nitrogen atoms were trans to the oxo and isopropoxo anions.[30] The V−O(maltol) bond lengths clearly indicate the extent of the trans effects of the oxo and methoxo ligands: the longest bond is the V−O linkage (V−O(6) = 2.252(2) Å) trans to the oxo ligand (stronger trans ligand), followed by the V−O bond (V−O(3) = 2.121(3) Å) trans to the methoxo ligand, while bonds between the two alkoxo oxygen atoms of the maltolato ligand and vanadium (V−O(5) = 1.910(2), V−O(2) = 1.943(3) Å) fall within the normal V−O single bond range.[31]

Oxidation Kinetics in MeOH. The kinetics of the oxidation of VO(ma)$_2$ by O$_2$ in MeOH were followed by quantitative UV−vis spectroscopy. A solution of *cis*-VO(OMe)(ma)$_2$ in MeOH is red with an absorption maximum at $\lambda = 448$ nm; this was selected to monitor the appearance of product. The suitable concentration was in the mM range because pseudo-first-order conditions were then readily achieved, the solubility of O$_2$ in MeOH at room temperature and 1 atm of O$_2$ being ∼7 mM.[32] As discussed above, the presence of excess ligand (a 20-fold excess of maltol was used) was crucial in order to suppress ligand dissociation processes. The rate constants are defined as in eq 1, where k_{obs} refers to the observed pseudo-first-order

$$\text{rate} = \frac{\mathrm{d}[\text{VO(OMe)(ma}_2)]}{\mathrm{d}t} = k_{obs}[\text{VO(ma)}_2] = k[\text{VO(ma)}_2][\text{O}_2] \quad (1)$$

rate constant and k to the second-order constant. Typical kinetic plots are shown in Figure 4. The logarithmic plot (Figure 4, inset) is linear for at least three half-lives, giving $k_{obs} = 1.81 \times 10^{-3}$ s^{-1} and $t_{1/2} = 383$ s (average of three runs) under the conditions noted. Varying only the concentration of VO(ma)$_2$ (between 0.2 and 0.4 mM, 3 runs) resulted in an identical rate constant, within experimental error.

The oxygen concentrations in the reaction solution were evaluated by measuring the total pressure of the system. The

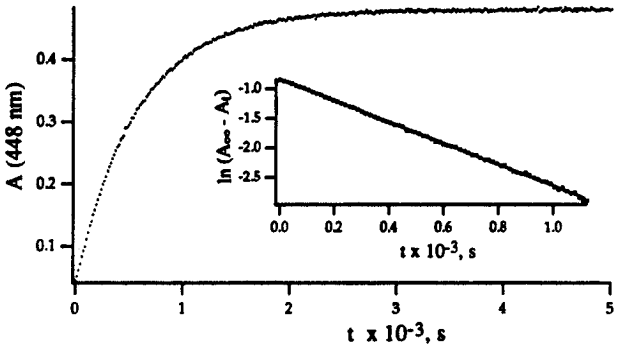

Figure 4. Oxidation of VO(ma)$_2$ in MeOH as a function of time. Inset: Semilogarithmic first order plot. Conditions: [VO(ma)$_2$] = 0.2 mM, [maltol] = 4 mM, P_{O_2} = 470 mmHg ([O$_2$] = 6.4 mM), T = 25 °C.

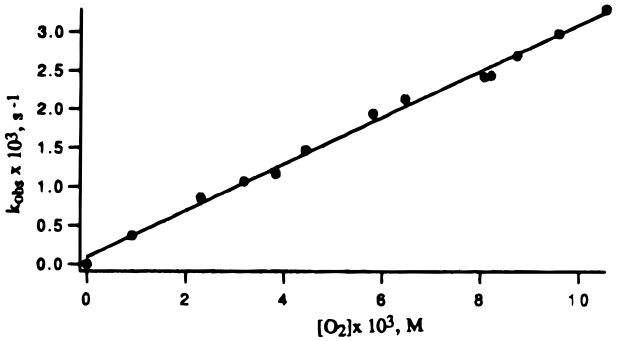

Figure 5. Plot of oxidation rate constants, k_{obs} vs [O$_2$]. Conditions: [VO(ma)$_2$] = 0.2 mM, [maltol] = 4 mM, 25 °C.

relationship $P_{total} = P_{O_2} + P_{MeOH}$ holds if the methanol solution is thoroughly degassed (by three cycles of freeze/pump/thaw). The MeOH vapor pressure (P_{MeOH}) at 25 °C was taken to be 121 mm Hg,[33] and then, based on Henry's law, the dioxygen concentrations were calculated based on literature data for the solubility of O$_2$ in MeOH.[32] At 25 °C, a plot of k_{obs} vs [O$_2$] yielded a straight line passing through the origin (Figure 5), indicating an overall second-order reaction. The second-order rate constant k was 0.31 M^{-1} s^{-1} at 25 °C.

VO(ma)$_2$ in Water. When the reaction medium is changed from MeOH to H$_2$O, the oxidation product of VO(ma)$_2$ changes from *cis*-VO(OMe)(ma)$_2$ to *cis*-[VO$_2$(ma)$_2$]$^-$, a complex of which the K$^+$ salt has been structurally characterized.[22] The diagnosis of the anonic vanadium(V) product (prepared by oxidizing VO(ma)$_2$ with O$_2$ in the presence of excess maltol) was based on the constant ^{51}V NMR chemical shift (−496 ppm) observed over a pH range of 5−8.5. The kinetics were monitored by spectrophotometric measurement of the appearance of the light yellow *cis*-[VO$_2$(ma)$_2$]$^-$, which had a broad absorption maximum at ∼400 nm, quite suitable for kinetic study. A 20-fold excess of maltol was used in all kinetic runs to prevent ligand dissociation. In the presence of excess ligand, the 4:1 VO(ma)$_2$:O$_2$ stoichiometry of the overall reaction was verified by an oxygen-uptake experiment. Because k_{obs} depends on pH (Scheme 2, *vide infra*), solutions were buffered. As reported by Crans *et al.*,[34] among the commercially available buffers for biological studies, Hepes interacts significantly neither with vanadate nor with vanadyl ions. Indeed, there were no detectable interactions of VO(ma)$_2$ or *cis*-[VO$_2$(ma)$_2$]$^-$ with Hepes in aqueous solution as examined independently by ESR

(30) Scheidt, W. R. *Inorg. Chem.* **1973**, *12*, 1758.
(31) Boas, L. V.; Pessoa, J. C. In *Comprehensive Coordination Chemistry*; Wilkinson, G., Gillard, R. D., McCleverty, J. A., Eds.; Pergamon Press: Oxford, England, 1987; Vol. 3; p 453.
(32) *Solubility Data Series*; Fogg, P. G. T., Young, C. L., Eds.; Pergamon Press: Oxford, England, 1981; Vol. 7, p 262.
(33) *CRC Handbook of Chemistry and Physics*; 64th ed.; Weast, R. C.; Astle, M. J.; Beyer, W. H., Eds.; CRC Press, Inc.: Boca Raton, FL, 1983.
(34) Crans, D. C.; Bunch, R. L.; Theisen, L. A. *J. Am. Chem. Soc.* **1989**, *111*, 7597.

Scheme 2. BMOV in Aerobic Aqueous Solution

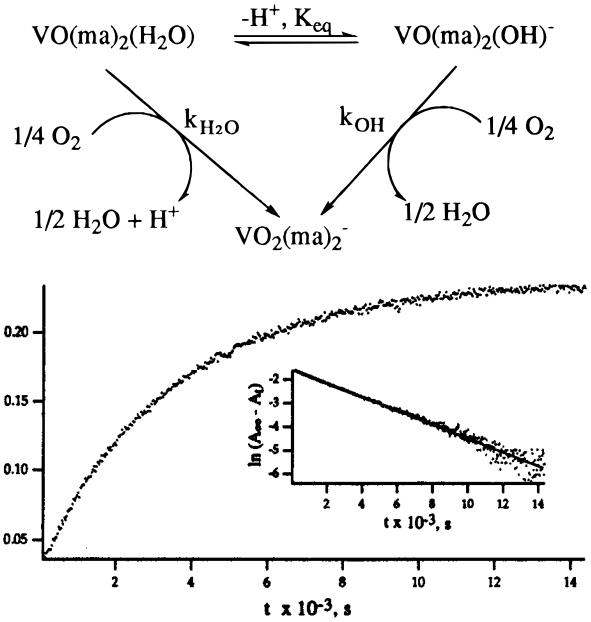

Figure 6. Oxidation of $VO(ma)_2$ in H_2O as a function of time (5 half-lives). Inset: Semilogarithmic first order plot. Conditions: $[VO(ma)_2]$ = 0.6 mM; [maltol] = 12 mM; P_{O_2} = 760 mmHg ($[O_2]$ = 1.27 mM); [Hepes] = 50 mM; pH = 7.5; T = 25 °C.

and ^{51}V NMR, respectively. With [Hepes] > 50 mM, the pH values of the buffer solutions were held constant within ±0.1 pH unit over the reaction period.

Oxidation Kinetics in Aqueous Solution. Compared to the absorption maximum of *cis*-$VO(OMe)(ma)_2$ (448 nm), that of *cis*-$[VO_2(ma)_2]^-$ is at 400 nm, and the corresponding molar absorptivity is less (ϵ = 3700 vs 400 M^{-1} cm^{-1}). Consequently, more concentrated $VO(ma)_2$ solutions (≥ 0.6 mM) were required for significant changes to be observed in the absorption intensity during an oxidation reaction. This, combined with the limited solubility of O_2 in H_2O (~1.3 mM at 1 atm of O_2), made it difficult to have the dissolved O_2 component in a large excess; however, pseudo-first-order conditions were achieved within the experimental procedure used. The total volume of the working cell (Figure 1) is ~50 mL, and only ~5 mL of solution was used in each kinetic run; thus the total oxygen in the cell (at 1 atm of O_2) is 2.3 mmol, approximately 3 orders of magnitude more than the concentration of $VO(ma)_2$ in solution. Consequently, the $[O_2]$ would remain effectively constant during the oxidation reaction, as long as the dissolution of O_2 into the liquid phase is fast compared to the reaction rate. Such conditions clearly hold as evidenced by the nature of the first-order plot (Figure 6) which was linear over at least three half-lives.

The dependence of the pseudo-first-order rate constants on oxygen concentration was also examined. At a given pH and temperature, an increase in oxygen partial pressure from 0.2 (1 atm air) to 1.0 atm increased k_{obs} by a factor of 5.0 ± 0.2 (four measurements), consistent with a first order dependence of k_{obs} on $[O_2]$. The measured second-order rate constant was 0.21 M^{-1} s^{-1} at pH = 7.25 and 25 °C.

No ESR signal other than that for $VO(ma)_2$[23] was detected at room temperature in monitoring the behavior of $VO(ma)_2$ in air-saturated aqueous solution, while successive ^{51}V NMR measurements of the same solution indicated the absence of any vanadium(V) peroxo species.[35]

pH Dependence. The pH dependence of k_{obs} was studied at constant reagent concentrations ($[VO(ma)_2]$ = 0.6 mM; [maltol] = 12 mM; P_{O_2} = 1 atm) over a pH range of 5.0−8.5. Studies outside this range were limited both by decomposition of the vanadium complexes and by the availability of noncoordinating buffers. The variation of ionic strengths of the buffer solutions at different pH was ignored in the evaluation of reaction rates, as a constant k_{obs} value was observed for reactions carried out under the same conditions with only the ionic strength (NaCl) varied (results not shown). Figure 7 shows the k_{obs} vs pH data, a standard S-type profile for reactivity via aquo and hydroxo species equilibrated via the pK_a expression for a coordinated water (Scheme 2 and eqs 2 and 3).

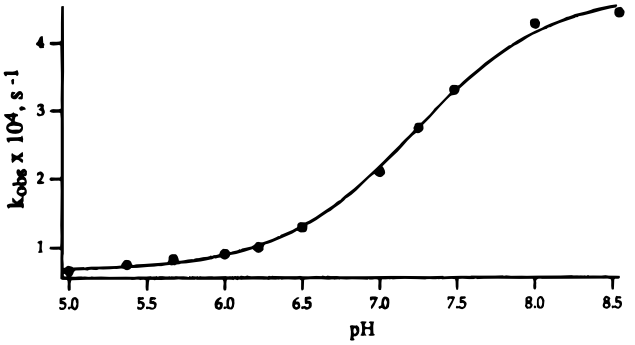

Figure 7. Plot of k_{obs} vs pH, dots from data, line from simulation. Conditions: $[VO(ma)_2]$ = 0.6 mM; [maltol] = 12 mM; P_{O_2} = 760 mm Hg ($[O_2]$ = 1.27 mM); [Hepes] = 50 mM; T = 25 °C.

Table 3. Second-Order Rate Constants for the Reactions of $[VO(ma)_2(OH)]^-$ and $VO(ma)_2(H_2O)$ with O_2 at Various Temperatures

T (°C)	18	25	40
k_{OH} (M^{-1} s^{-1})	0.214	0.394	1.234
k_{H_2O} (M^{-1} s^{-1})	0.036	0.080	0.249

$$\text{rate} = \frac{d[VO_2(ma)_2]^-}{dt} = k_{H_2O}[VO(ma)_2(H_2O)][O_2] + k_{OH}[VO(ma)_2(OH)^-][O_2] \quad (2)$$

$$= k_{obs}^{H_2O}[VO(ma)_2(H_2O)] + k_{obs}^{OH}[VO(ma)_2(OH)^-]$$

This leads to the standard expression:

$$k_{obs} = \frac{k_{obs}^{H_2O}[H^+] + k_{obs}^{OH}K_{eq}}{K_{eq} + [H^+]} \quad (3)$$

A computer-assisted fitting of the observed 25 °C data (Figure 7, dots) to equation 3 (Figure 7, line) yielded K_{eq}, $k_{obs}^{H_2O}$, and k_{obs}^{OH} values of 5.7 × 10^{-8}, 6.6 × 10^{-5} s^{-1}, and 4.7 × 10^{-4} s^{-1}, respectively. The K_{eq} value corresponds to a pK_a value of 7.2. Although a direct measurement of pK_a for the coordinated water in $VO(ma)_2(H_2O)$ was not made, pK_a values of related oxovanadium(IV) complexes have appeared in the literature: $[VO(nta)(H_2O)]^-$ (pK_a = 6.9, nta^{3-} = nitrilotriacetate, an O_3N donor ligand),[36] and $[VO(pmida)(H_2O)]$ (pK_a = 6.4, $pmida^{2-}$ = (2-pyridylmethyl)iminodiacetate, an N_2O_2 donor ligand).[37] A pK_a of 7.2 for $VO(ma)_2(H_2O)$ which contains an O_4 ligand donor set seems appropriate.

Temperature Dependence. Second-order rate constants derived for both k_{H_2O} and k_{OH} pathways were measured for the oxidation reaction of $VO(ma)_2$ in aqueous solution at various

(35) Butler, A.; Clague, M. J.; Meister, G. E. *Chem. Rev.* **1994**, *94*, 625.
(36) Nishizawa, M.; Saito, K. *Inorg. Chem.* **1980**, *19*, 2284.
(37) Ooi, S.; Nishizawa, M.; Saito, K.; Kuroya, H.; Saito, K. *Bull. Chem. Soc. Jpn.* **1977**, *52*, 452.

Scheme 3. Proposed Mechanism

$$VO(ma)_2 + O_2 \xrightarrow{k_1} VO(ma)_2(O_2)$$

$$VO(ma)_2(O_2) + VO(ma)_2 \xrightarrow{k_2} VO(ma)_2(\mu\text{-}OO)VO(ma)_2$$

$$VO(ma)_2(\mu\text{-}OO)VO(ma)_2 + 2MeOH \xrightarrow{k_3} VO(OMe)(ma)_2 + H_2O_2$$

$$H_2O_2 \longrightarrow 1/2\ O_2 + H_2O$$

Net reaction:

$$2\ VO(ma)_2 + 1/2\ O_2 + 2\ MeOH \longrightarrow 2VO(OMe)(ma)_2 + H_2O$$

temperatures . Table 3 summaries the rate constant values; the limited data gave excellent linearity with Eyring plots from which the following activation parameters were evaluated: k_{H_2O} ($\Delta H^{\ddagger} = 63 \pm 6$ k J mol^{-1}, $\Delta S^{\ddagger} = -55 \pm 20$ J K^{-1} mol^{-1}); k_{OH} ($\Delta H^{\ddagger} = 58 \pm 1$ k J mol^{-1}, $\Delta S^{\ddagger} = -60 \pm 3$ J K^{-1} mol^{-1}).

Discussion

Kinetic studies of V(IV)/V(V) redox reactions of "uncomplexed" vanadium salts have been largely limited because of the ease of their hydrolysis and oligomerization; chelating ligands play an important role in stabilizing V(IV), and especially V(V) complexes against these processes. The oxidation of $VO(ma)_2$ by molecular oxygen is straightforward in both H_2O and MeOH media, as long as excess maltol is present. Thus, in the presence of 20-fold excess maltol and a pH of 5−8.5, the oxovanadium moiety forms exclusively monomeric 1:2 (metal to ligand) species in both oxidation states +4 and +5, as confirmed by ESR and ^{51}V NMR spectroscopies, as well as by the identities of solid state structures of *cis*-VO(OMe)-$(ma)_2$ (this work) and *cis*-K[$VO_2(ma)_2$]·H_2O.[22]

The primary objective in carrying out this study was to examine the stability of the insulin mimetic compound BMOV ($VO(ma)_2$) in aqueous solution under various conditions. The oxidation of $VO(ma)_2$ by O_2 in a non-aqueous medium (MeOH) was studied initially as a model reaction, because the corresponding reaction in H_2O was complicated by a pH-dependence.

Although the net reaction in MeOH is straightforward stoichiometrically, the oxidation of $VO(ma)_2$ by dioxygen is a complex multistep reaction. The observed rate law (eq 1) and the stoichiometry are consistent with the mechanism proposed in Scheme 3 (any solvent coordination has been omitted), where the k_1 step (formation of a dioxygen species, presumably a V^V-end-on superoxo complex) is rate determining; the subsequent steps (k_2 and k_3), involving formation of a bridged peroxide-V^V intermediate and cleavage of the O−O bridge by MeOH, are rapid. Alternatively the presumed superoxide species could react directly with MeOH to generate the V^V product. In either case subsequent decomposition of peroxide to water and oxygen or disproportionation of superoxide to oxygen and peroxide (and subsequent decomposition of the latter), reactions which are necessary to account for the 4:1 V^{IV}−O_2 stoichiometry, do not appear to interfere with the observed simple kinetics (see below).

The oxidation of $VO(ma)_2$ by O_2 in aqueous solution is believed to proceed similarly to that in MeOH solution; the corresponding product would be $VO(ma)_2(OH)$ which deprotonates ($pK_a \sim 2$[22]) to give the observed product *cis*-[VO_2-$(ma)_2$]$^-$. From the k_{obs}−pH dependence, the anionic species [$VO(ma)_2(OH)$]$^-$ was found to be ∼7 times more reactive toward O_2 than the neutral protonated form. This observation can be understood from an electronic point of view, in that the more negative charge on the complex in [$VO(ma)_2(OH)$]$^-$ should destabilize V(IV) with respect to V(V). The relatively low activation enthalpies $\Delta H^{\ddagger}$ of 63 and 58 kJ mol^{-1} determined for the $VO(ma)_2(H_2O)$ and [$VO(ma)_2(OH)$]$^-$ pathways, respectively (Scheme 2), are not much different from the values reported for the anation reactions in water between VO(pmida)-(H_2O) (aquaoxo((2-pyridylmethyl)iminodiacetato)vanadium(IV)) and the NCS^- (48.9 ± 1.7 kJ mol^{-1}) or N_3^- (47.2 ± 6 kJ mol^{-1}) anions, where an associative mechanism was suggested.[38] The respective $\Delta S^{\ddagger}$ values (−55, −60 J K^{-1} mol^{-1}) are negative, as expected for a simple bimolecular addition.

The electronic configuration (d^1) and formally unsaturated coordination environment of VOL_2 complexes may invoke a radical-like behavior at the metal center, as noted by Pasquali *et al.*[39] in studying the reactivity of VOQ_2 (Q = 8-quinolinato) toward dioxygen and related oxidizing agents. The proposed coordination of O_2 directly to the vanadium center was based on such properties of the V(IV) moiety, and the fact that similar coordination is known for many other paramagnetic (radical) transition metal complexes.[40−42] We are uncertain as to whether any coordinated solvent dissociates upon O_2 association with the metal center, because seven-coordinate vanadium(V) complexes are known.[31] The necessary electron-transfer would then proceed via an inner-sphere pathway, and the electronic environment around the metal is expected to influence the rate of the electron-transfer, and possibly the rate of the overall reaction, although the association of O_2 is the preferred rate-determining step.

The failure to detect any presumed $V^V(O_2^{\bullet})$ radicals by ESR spectroscopy is probably due to their extremely short half-lives at room temperature, and indeed we postulate a relatively rapid removal of such species via the k_2 step (Scheme 3). We consider the formation of any vanadium(V) peroxides (by side-on coordination of O_2 to a vanadium(III) center[43]) to be highly unlikely, because these complexes are commonly quite stable, and are easily distinguishable from other oxovanadium(V) moieties by ^{51}V NMR spectra;[35] there is also no obvious route available for formation of vanadium(III) in an ambient environment. Further, the H_2O_2-oxidation reaction of uncomplexed VO^{2+}(aq) has been studied, and an unidentified oxygen-radical species was suggested as one of the intermediates.[44,45]

In contrast to the stoichiometries measured in our studies, oxygen consumption studies by Ravi Shankar and Ramasarma[44] indicated that oxygen reduction by vanadyl sulfate generates H_2O_2. In an effort to substantiate further the proposed mechanism outlined in Scheme 3, we studied the redox reaction between $VO(ma)_2$ and H_2O_2 for possible Fenton type chemistry. The assumptions that the H_2O_2 generated is nonaccumulating and that it subsequently oxidizes only $VO(ma)_2$ species were further tested as follows. The oxidation of 0.2 mM $VO(ma)_2$ by 0.2 mM H_2O_2 was at least an order of magnitude faster than the oxidation by 7 mM O_2, which suggests that H_2O_2, if present, can only be at a (small) steady-state concentration. In examining whether the proposed H_2O_2 intermediate would oxidize the excess maltol molecules present, we found no differences in the ^{1}H NMR spectra of the reaction mixture (with or without)

(38) Nishizawa, M.; Saito, K. *Inorg. Chem.* **1978**, *17*, 3676.
(39) Pasquali, M.; Landi, A.; Floriani, C. *Inorg. Chem.* **1979**, *18*, 2397.
(40) Feig, A. L.; Lippard, S. J. *Chem. Rev.* **1994**, *94*, 759.
(41) Kang, C.; Anson, F. C. *Inorg. Chem.* **1995**, *34*, 2771.
(42) Sawyer, D. T. *Oxygen Chemistry*; Oxford University Press: New York, 1991.
(43) Chandrasekhar, P.; Wheeler, R. A.; Hoffmann, R. *Inorg. Chim. Acta* **1987**, *129*, 51.
(44) Ravi Shankar, H. N.; Ramasarma, T. *Mol. Cell. Biochem.* **1993**, *129*, 9.
(45) Ravishankar, H. N.; Chaudhuri, M. K.; Ramasarma, T. *Inorg. Chem.* **1994**, *33*, 3788.

an addition of H_2O_2; the finding is also consistent with the observed 4:1 $VO(ma)_2$:O_2 stoichiometry.

Finally, the proposed mechanism is consistent with the observed independence of the rate on ionic strength, because a reaction involving a neutral molecule (in this case O_2) should have a rate largely uninfluenced by ionic strength.[46]

The observed second order rate constant of the $VO(ma)_2/O_2$ reaction in aqueous solution at pH = 7.25, T = 25 °C (eq 3) is 0.21 M^{-1} s^{-1}, comparable with the value of 0.31 M^{-1} s^{-1} obtained for the same reaction in MeOH at the same temperature. However, because of its nonpolar nature, dioxygen is less soluble in water than in MeOH (∼1.3 mM vs ∼7 mM at 1 atm O_2), and consequently the rates of aerial oxidation of $VO(ma)_2$ at 25 °C in aqueous solution (pH ∼ 7) will be about 8 times less than in MeOH. In view of the low oxygen tension in biological systems, the observed kinetic data suggest that when $VO(ma)_2$ is administered, the tetravalent vanadium is most likely the dominant species absorbed. The existence of endogenous reducing agents (glutathione, etc.) in biological systems adds further support to the above conclusion, as ascorbic acid was found to inhibit substantially the oxidation of $VO(ma)_2$ in aqueous solution.[22]

Acknowledgment is made to the Natural Sciences and Engineering Research Council of Canada for a postdoctoral fellowship (Y.S.) and a research grant (B.R.J.), to the Medical Research Council of Canada for an operating grant (C.O.), to Edward Shuter and Terrance Wong for initial assistance with experimental procedures, and to Dr. Yu Wang for the O_2-uptake experiments.

Supporting Information Available: Complete tables of crystallographic data, atomic coordinates, hydrogen atom parameters, anisotropic displacement parameters, torsion angles, intermolecular contacts, and least-squares planes (16 pages). See ordering information on any current masthead page.

IC951452T

(46) Wilkins, R. G. *Kinetics and Mechanism of Reactions of Transition Metal Complexes;* 2nd ed.; VCH Publishers, Inc.: New York, 1991; p 465.